Hindawi
Journal of Applied Mathematics
Volume 2018, Article ID 6835179, 5 pages
https://doi.org/10.1155/2018/6835179

Research Article

Analytical Approach for Solving the Internal Waves Problems Involving the Tidal Force

Jaharuddin[1] **and Hadi Hermansyah**[2]

[1]*Department of Mathematics, Faculty of Mathematics and Natural Sciences, Bogor Agricultural University, Bogor, West Java 16680, Indonesia*
[2]*Department of Mechanical Engineering, Balikpapan State Polytechnic, Balikpapan, East Borneo 76126, Indonesia*

Correspondence should be addressed to Jaharuddin; jaharmath@gmail.com

Received 23 April 2018; Accepted 10 July 2018; Published 7 August 2018

Academic Editor: Jian G. Zhou

The mathematical model for describing internal waves of the ocean is derived from the assumption of ideal fluid; i.e., the fluid is incompressible and inviscid. These internal waves are generated through the interaction between the tidal currents and the basic topography of the fluid. Basically the mathematical model of the internal wave problem of the ocean is a system of nonlinear partial differential equations (PDEs). In this paper, the analytical approach used to solve nonlinear PDE is the Homotopy Analysis Method (HAM). HAM can be applied to determine the resolution of almost any internal wave problem involving tidal forces. The use of HAM in the solution to basic fluid equations is efficient and simple, since it involves only modest calculations using the common integral.

1. Introduction

Internal waves are gravitational waves that exist on two layers of fluid having different densities. Internal waves are formed due to a meeting among layers of seawater that have different densities of generating forces coming from wind, tide, or even movement of ships. The density difference causes the seawater to become layered where water with a larger density will be below that with a smaller density. This condition stimulates the formation of boundary of the two layers fluid (interfaces) where in case of external disturbance (by the existing generating force), an interlayer wave occurs without affecting the waves on the surface. Generating internal waves requires a large force, for instance, generated by the interaction of strong tidal currents, fluid coating, and lower topography. Research on internal waves at sea has previously been applied to various applications and ranges, for example, to detect the strength of offshore oil platform pylons [1] and to measure how the impact of internal waves can affect *Chlorophila* [2]. In addition, this wave can also affect the marine habitat that is the spatial distribution of *Planktothrix rubescens* [3].

Internal waves of the ocean can be modeled in terms of mathematical equations using the ideal fluids assumptions (incompressible and inviscid) of mass conservation laws and the law of momentary vapor. Internal waves are generated through the interaction between the tidal flow and the topography in a nonuniform fluid layer by solving the Navier-Stokes equation in Boussinesq approximation. Basically the mathematical representation of the internal waves of the ocean is a system of nonlinear partial differential equations (PDEs) [4]. In many cases, nonlinear PDE systems are very difficult to be resolved analytically. Thus an analytic approach can provide a solution which is almost needed.

The analytical approach for solving the nonlinear PDEs was first introduced by Liao in 1992, i.e., the homotopy analysis method (HAM). HAM excellence lies in the selection mechanism of initial values and auxiliary parameters so as to extend the convergence region [5]. Earlier version of HAM methods has been applied for various nonlinear problem solving such as the Klein-Gordon equation [6], El Nino Southern Oscillation [7], Huxley [8], Zakharov-Kuznetsov equation [9], and one species growth model in the polluted environment [10]. In this article, we review the internal

wave issues in the sea that involve tidal forces using the HAM method. The completion of almost this method will be compared to the numerical settlement of error calculations and graphical visualization of the settlement.

The equation used in this study is the Navier-Stokes equation with Boussinesq approximation, in which it is assumed that the internal waves are generated by the interaction between pairs of currents with two-dimensional topography in a nonuniform fluid layer. In this model, ρ is the density, ρ_0 a reference density, p pressure, and u and w velocity, respectively, in the horizontal and vertical directions

$$\begin{aligned} \frac{\partial u}{\partial t} + u\frac{\partial u}{\partial x} + g\frac{\partial \eta}{\partial x} - \nu\frac{\partial^2 u}{\partial x^2} - \frac{F_{tide}}{\rho_0} &= 0, \\ \frac{\partial w}{\partial t} + u\frac{\partial w}{\partial x} + \frac{g\rho}{\rho_0} + gH - \frac{F_{tide}}{\rho_0} &= 0, \\ \frac{\partial \eta}{\partial t} + u\frac{\partial \eta}{\partial x} + wH + \eta\frac{\partial u}{\partial x} &= 0, \end{aligned} \tag{1}$$

where t is time, η is the fluid depth, g is the constant of gravity, H represents the mean of fluid depth, ν is the kinematic viscosity, and F_{tide} is the tidal force given by

$$F_{tide} = \rho_0 A\omega^2 \sin \omega t. \tag{2}$$

In (2), A is tidal excursion and it was found that the value of A was less than 10% variation in the measured quantities of this range; the data presented are for $A = 20$ m; ω is the tidal frequency. Another parameter is the height caused by the change in horizontal directional pressure formulated by $H = -(f/g)\overline{U}$, where $\overline{U} = 2.5$ m/s and the Coriolis parameter $f = 2\Omega \sin(\alpha)$ depending on the angular velocity earth rotation Ω.

2. Analysis Method

In this part we illustrate the concept of homotopy method. Suppose that a nonlinear equation is given in the form as below:

$$\mathcal{N}[u(x,t)] = 0, \tag{3}$$

where $\mathcal{N}$ is a nonlinear derivative operator, $u(x,t)$ is an unknown function, x and t are independent variables, and $\mathcal{L}$ is defined as linear operator which satisfies

$$\mathcal{L}[f(x,t)] = 0, \quad \text{when } f(x,t) = 0. \tag{4}$$

Let $u_0(x,t)$ be the initial approach of solving (3); $q \in [0,1]$ is an embedding parameter, $\hbar$ is auxiliary parameter, and $A(x)$ is an additional function. In the frame of the homotopy method, we first construct such a continuous variation (or deformation) $\phi(x,t;q)$ that as q increases from 0 to 1, $\phi(x,t;q)$ varies from the initial approach $u_0(x,t)$ to the solution $u(x,t)$ of (3). Such kind of continuous variation (or mapping) is governed by the so-called zero-order deformation equation

$$\begin{aligned} &(1-q)\mathcal{L}[\phi(x,t;q) - u_0(x,t)] \\ &\quad = q\hbar A(x)\mathcal{N}[\phi(x,t;q)]. \end{aligned} \tag{5}$$

At $q = 0$, the zero-order deformation equation (5) becomes

$$\mathcal{L}[\phi(x,t;0) - u_0(x,t)] = 0, \tag{6}$$

such that

$$\phi(x,t;0) = u_0(x,t). \tag{7}$$

When $q = 1$ and $\hbar \neq 0$, then the zero-order deformation equation (5) becomes

$$\mathcal{N}[\phi(x,t;1)] = 0, \tag{8}$$

which is exactly the same as the original equation (3), provided

$$\phi(x,t;1) = u(x,t). \tag{9}$$

Thus, as q increases from 0 to 1, the solution $\phi(x,t;q)$ varies continuously from the initial approach $u_0(x,t)$ to the exact solution $u(x,t)$. So, (5) defines a homotopy of function $(x,t;q) : u_0(x,t) \sim u(x,t)$. Such kind of continuous variation is called deformation in topology, and this is the reason why we call (5) the zero-order deformation equation. By using the Taylor expansion from $\phi(x,t;q)$ to q, the following is obtained

$$\phi(x,t;q) = u_0(x,t) + \sum_{m=1}^{\infty} u_m(x,t)\, q^m, \tag{10}$$

where

$$u_m(x,t) = \frac{1}{m!}\frac{\partial^m \phi(x,t;q)}{\partial q^m}\bigg|_{q=0}. \tag{11}$$

Suppose that given the initial value of $u_0(x,t)$, the linear operator $\mathcal{L}$ and the auxiliary parameters $\hbar$ are not equal to zero and the auxiliary function $A(x)$ is chosen so that (10) is from $\phi(x,t;q)$ convergent at $q = 1$. Hence, we may assume the following series solution:

$$u(x,t) = \phi(x,t;1) = u_0(x,t) + \sum_{m=1}^{+\infty} u_m(x,t). \tag{12}$$

According to (10), (5) can be rewritten as follows:

$$\begin{aligned} &(1-q)\mathcal{L}\left[\sum_{m=1}^{\infty} u_m(x,t)\, q^m\right] \\ &\quad = q\hbar A(x)\mathcal{N}[\phi(x,t;q)], \end{aligned} \tag{13}$$

such that

$$\begin{aligned} &\mathcal{L}\left[\sum_{m=1}^{\infty} u_m(x,t)\, q^m\right] - q\mathcal{L}\left[\sum_{m=1}^{\infty} u_m(x,t)\, q^m\right] \\ &\quad = q\hbar A(x)\mathcal{N}[\phi(x,t;q)]. \end{aligned} \tag{14}$$

By deriving (14) as much as m times with respect to q, then the following is obtained:

$$\begin{aligned} &m!\mathcal{L}[u_m(x,t) - u_{m-1}(x,t)] \\ &\quad = \hbar A(x)\, m\frac{\partial^{m-1}\mathcal{N}[\phi(x,t;q)]}{\partial q^{m-1}}\bigg|_{q=0}, \end{aligned} \tag{15}$$

such that

$$\begin{aligned}&\mathscr{L}\left[u_m(x,t)-\chi_m u_{m-1}(x,t)\right]\\&\quad=\hbar A(x)\,\mathfrak{R}_m\left(u_{m-1}(x,t)\right),\end{aligned}\tag{16}$$

where

$$\mathfrak{R}_m\left(u_{m-1}(x,t)\right)=\frac{1}{(m-1)!}\left.\frac{\partial^{m-1}\mathcal{N}\left[\phi(x,t;q)\right]}{\partial q^{m-1}}\right|_{q=0}\tag{17}$$

and

$$\chi_m=\begin{cases}0 & m\le 1,\\ 1 & m>1.\end{cases}\tag{18}$$

3. Application of HAM

In this section we discuss the use of homotopy method to explain the internal wave motion with finite depth. The linear operation in the homotopy method is defined as follows:

$$\mathscr{L}_i\left[\phi_i(x,t;q)\right]=\frac{\partial\phi_i(x,t;q)}{\partial t},\quad i=1,2,3.\tag{19}$$

Based on the system in (1), we may have the following linear operators:

$$\begin{aligned}\mathcal{N}_1\left[\phi_1,\phi_2,\phi_3\right]&=\frac{\partial\phi_1}{\partial t}+\phi_1\frac{\partial\phi_1}{\partial x}+g\frac{\partial\phi_3}{\partial x}-\nu\frac{\partial^2\phi_1}{\partial x^2}\\&\quad-\frac{F_{tide}}{\rho_0}\\\mathcal{N}_2\left[\phi_1,\phi_2,\phi_3\right]&=\frac{\partial\phi_2}{\partial t}+\phi_1\frac{\partial\phi_2}{\partial x}+\frac{g\rho}{\rho_0}+gH-\frac{F_{tide}}{\rho_0},\\\mathcal{N}_3\left[\phi_1,\phi_2,\phi_3\right]&=\frac{\partial\phi_3}{\partial t}+\phi_1\frac{\partial\phi_3}{\partial x}+\phi_2H+\phi_3\frac{\partial\phi_1}{\partial x}.\end{aligned}\tag{20}$$

Now, the zero-order deformation equation is as follows:

$$\begin{aligned}&(1-q)\,\mathscr{L}_1\left[\phi_1(x,t;q)-u_0(x,t)\right]\\&\quad=q\hbar_1\mathcal{N}_1\left[\phi_1,\phi_2,\phi_3\right]\\&(1-q)\,\mathscr{L}_2\left[\phi_2(x,t;q)-w_0(x,t)\right]\\&\quad=q\hbar_2\mathcal{N}_2\left[\phi_1,\phi_2,\phi_3\right]\\&(1-q)\,\mathscr{L}_3\left[\phi_3(x,t;q)-\eta_0(x,t)\right]\\&\quad=q\hbar_3\mathcal{N}_3\left[\phi_1,\phi_2,\phi_3\right].\end{aligned}\tag{21}$$

According to (21), when $q=0$ we can write

$$\begin{aligned}\phi_1(x,t;0)&=u_0(x,t)=u(x,0),\\\phi_2(x,t;0)&=w_0(x,t)=w(x,0),\\\phi_3(x,t;0)&=\eta_0(x,t)=\eta(x,0),\end{aligned}\tag{22}$$

and when $q=1$, we have

$$\begin{aligned}\phi_1(x,t;1)&=u(x,t),\\\phi_2(x,t;1)&=w(x,t),\\\phi_3(x,t;1)&=\eta(x,t).\end{aligned}\tag{23}$$

Thus, we obtain the m^{th}-order deformation equation:

$$\begin{aligned}&\mathscr{L}_1\left[u_m(x,t)-\chi_m u_{m-1}(x,t)\right]\\&\quad=\hbar_1R_{1,m}\left[\vec{u}_{m-1},\vec{w}_{m-1},\vec{\eta}_{m-1}\right],\\&\mathscr{L}_2\left[w_m(x,t)-\chi_m w_{m-1}(x,t)\right]\\&\quad=\hbar_2R_{2,m}\left[\vec{u}_{m-1},\vec{w}_{m-1},\vec{\eta}_{m-1}\right],\\&\mathscr{L}_3\left[\eta_m(x,t)-\chi_m\eta_{m-1}(x,t)\right]\\&\quad=\hbar_3R_{3,m}\left[\vec{u}_{m-1},\vec{w}_{m-1},\vec{\eta}_{m-1}\right],\end{aligned}\tag{24}$$

where

$$\begin{aligned}\vec{u}_m&=\left(u_0(x,t),u_1(x,t),u_2(x,t),\ldots,u_m(x,t)\right),\\\vec{w}_m&=\left(w_0(x,t),w_1(x,t),w_2(x,t),\ldots,w_m(x,t)\right),\\\vec{\eta}_m&=\left(\eta_0(x,t),\eta_1(x,t),\eta_2(x,t),\ldots,\eta_m(x,t)\right).\end{aligned}\tag{25}$$

Now, the solution of the m^{th}- order deformation equation (24) for $m\ge 1$ becomes

$$\begin{aligned}u_m(x,t)&=\chi_m u_{m-1}(x,t)\\&\quad+\hbar_1\int_0^t R_{1,m}\left(\vec{u}_{m-1},\vec{w}_{m-1},\vec{\eta}_{m-1}\right)ds\\w_m(x,t)&=\chi_m w_{m-1}(x,t)\\&\quad+\hbar_2\int_0^t R_{2,m}\left(\vec{u}_{m-1},\vec{w}_{m-1},\vec{\eta}_{m-1}\right)ds\\\eta_m(x,t)&=\chi_m\eta_{m-1}(x,t)\\&\quad+\hbar_3\int_0^t R_{3,m}\left(\vec{u}_{m-1},\vec{w}_{m-1},\vec{\eta}_{m-1}\right)ds,\end{aligned}\tag{26}$$

where

$$\begin{aligned}&R_{1,m}\left(\vec{u}_{m-1},\vec{w}_{m-1},\vec{\eta}_{m-1}\right)\\&\quad=\frac{\partial u_{m-1}}{\partial t}+\sum_{n=0}^{m-1}u_n\frac{\partial u_{m-1-n}}{\partial x}+g\frac{\partial\eta_{m-1}}{\partial x}-\nu\frac{\partial^2u_{m-1}}{\partial x^2}\\&\qquad-\frac{F_{tide}}{\rho_0}\end{aligned}$$

$$R_{2,m}\left(\vec{u}_{m-1}, \vec{w}_{m-1}, \vec{\eta}_{m-1}\right) = \frac{\partial w_{m-1}}{\partial t} + \sum_{n=0}^{m-1} u_n \frac{\partial w_{m-1-n}}{\partial x} + \frac{g\rho}{\rho_0} + gH - \frac{F_{tide}}{\rho_0}$$

$$R_{3,m}\left(\vec{u}_{m-1}, \vec{w}_{m-1}, \vec{\eta}_{m-1}\right) = \frac{\partial \eta_{m-1}}{\partial t} + \sum_{n=0}^{m-1} u_n \frac{\partial \eta_{m-1-n}}{\partial x} + \eta_n \frac{\partial u_{m-1-n}}{\partial x} + w_{m-1} H. \tag{27}$$

According to (10) and (18) we have

$$u(x,t) = u_0(x,t) + \sum_{m=1}^{+\infty} u_m(x,t),$$
$$w(x,t) = w_0(x,t) + \sum_{m=1}^{+\infty} w_m(x,t), \tag{28}$$
$$\eta(x,t) = \eta_0(x,t) + \sum_{m=1}^{+\infty} \eta_m(x,t).$$

Furthermore, the initial settlement approach is chosen based on the completion of the current wave from the Navier-Stokes equation obtained by the following equation:

$$u_0(x,t) = \omega A \cosh(kx - \omega t),$$
$$w_0(x,t) = \omega A \sinh(kx - \omega t), \tag{29}$$
$$\eta_0(x,t) = A \cosh(kx - \omega t).$$

For simplification, then select $\hbar_1 = \hbar_2 = \hbar_3$. Further, the boundary conditions used in the solution of (1) are a polynomial determined by the settlement of HAM. The solution of (1) is numerically determined with the aid of a symbolic computing program. The resulting numerical settlement will be compared to the almost-resultant settlement with the HAM. The parameters used for the evaluation need the inclusion of the tidal force parameter $F_{tide} = \rho_0 A\omega^2 \sin \omega t$, where A is the tidal excursion; in this case A should be less than the channel width ($A = 20$ m) $\rho_0 = 1000\,\text{kg/m}^3$; $\nu = 0.01\,\text{m}^2/\text{s}$ is kinematic viscosity, tidal frequency ($\omega = \omega_{M2} = 1.4052 \times 10^{-4}$ rad/s), and earth's rotational angle velocity $\Omega = 7.29 \times 10^{-5}$ and $\alpha = \pi/3$ as the constant geostrophic current velocity. Furthermore there is also a constant of gravity $g = 9.8\,\text{m/s}^2$.

In the HAM application, the completion of high-order deformation is determined by (26). The completion of the high-order deformation obtained is the basis of determining the completion of the series. The result of series completion is a function that depends on the values of x and t. In this section, the completion of the obtained series is evaluated at a certain x and t value to determine the completion of the HAM. Nearly obtained solutions compared to their numerical settlement of the calculation of absolute error and visualization of the completion graph.

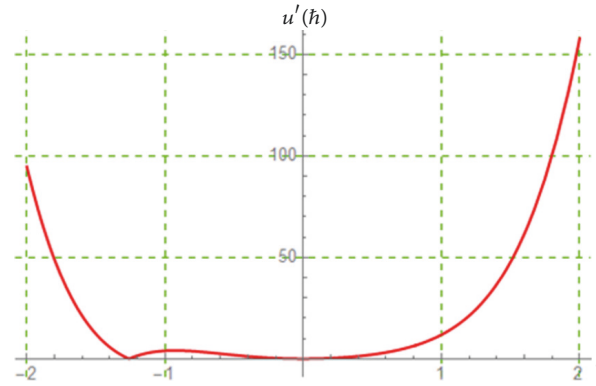

Figure 1: The $\hbar$-curves.

Based on the initial approach to (29) and given parameters, the following high-order deformation solutions are obtained:

$$\begin{aligned}
u_0(x,t) &= \omega A \cosh(kx - \omega t),\\
u_1(x,t) &= \hbar\,(-0.00002t \cosh(0.005t - 0.2x)\\
&\quad - 0.00025t \sinh(0.005t) - 19.59975t\\
&\quad \cdot \sinh(0.005t - 0.2x) - 0.0005t\\
&\quad \cdot \cosh(0.005t - 0.2x) \sinh(0.005t - 0.2x)),\\
w_0(x,t) &= \omega A \sinh(kx - \omega t),\\
w_1(x,t) &= \hbar\left(0.0001975t - 0.00025t\right.\\
&\quad \cdot \cosh(0.005t - 0.2x)\\
&\quad + 0.0005t \cosh(0.005t - 0.2x)^2 - 0.00025t\\
&\quad \left.\cdot \sinh(0.005t) + \frac{10133.2t}{1034}\right),\\
\eta_0(x,t) &= A \cosh(kx - \omega t),\\
\eta_1(x,t) &= \hbar\,(0.05t \sinh(0.005t - 0.2x)\\
&\quad - 0.2t\cosh(0.005t - 0.2x) \sinh(0.005t - 0.2x)),
\end{aligned} \tag{30}$$

and so on. The rest of the components of the iteration formulas by HAM can easily be obtained by symbolic computation software. Thus, we obtain the following approximate solution in term of a series up to third order:

$$\begin{aligned}
u(x,t) &= u_0(x,t) + u_1(x,t) + \cdots + u_3(x,t)\\
w(x,t) &= w_0(x,t) + w_1(x,t) + \cdots + w_3(x,t)\\
\eta(x,t) &= \eta_0(x,t) + \eta_1(x,t) + \cdots + \eta_3(x,t)
\end{aligned} \tag{31}$$

Note that (31) contains the auxiliary parameter $\hbar$. To obtain an appropriate range for $\hbar$, we consider the $\hbar$-curves. Based on Figure 1 we get the value of $\hbar = -1$.

Table 1: An absolute error between the numerical and HAM solution at $x = 0.1$ and $0 \leq t \leq 1$.

t	$\lvert u_{\text{HAM}} - u_{\text{NUM}} \rvert$	$\lvert w_{\text{HAM}} - w_{\text{NUM}} \rvert$	$\lvert \eta_{\text{HAM}} - \eta_{\text{NUM}} \rvert$
0	0	0.000027	0
0.1	2.039×10^{-6}	2.349×10^{-5}	6.708×10^{-6}
0.2	4.279×10^{-6}	2.001×10^{-5}	1.111×10^{-5}
0.3	6.644×10^{-6}	1.675×10^{-5}	1.503×10^{-5}
0.4	9.168×10^{-6}	1.286×10^{-5}	2.679×10^{-5}
0.5	1.186×10^{-5}	4.272×10^{-6}	7.368×10^{-5}
0.6	1.473×10^{-5}	1.963×10^{-5}	2.242×10^{-5}
0.7	1.778×10^{-5}	8.011×10^{-5}	6.218×10^{-5}
0.8	2.101×10^{-5}	2.143×10^{-4}	1.532×10^{-3}
0.9	2.443×10^{-5}	4.810×10^{-4}	3.406×10^{-3}
1	2.806×10^{-5}	9.682×10^{-4}	6.953×10^{-3}

The comparison of the results of the homotopy analysis method and numerical solution is given in Table 1. The explicit Runge-Kutta method in symbolic computation package has been used to find numerical solution of u, w, and η. Table 1 shows the absolute error between the HAM and the numerical solution for $\hbar = -1$, $x = 0.1$, and $0 \leq t \leq 1$. Based on Table 1, it is found that, in the HAM, the approximate solution has a small absolute error against the numerical settlement evaluated at a certain independent variable value. It can be seen in the table that there exists a very good agreement between HAM result and numerical solutions.

The generation of internal waves by tidal force occurs in the stratified fluid when propagation of barotropic tidal currents interacts with rough surface topography, resulting in vertical movement and of local internal pressure. These local perturbations propagate as waves which are far from the center of generation. Internal wave plays an important role for transferring energy to the deep sea turbulence. When barotropic tidal currents flow on a rough topography sill, part of barotropic energy will vanish directly through dissipation and local mixing, and other part of barotropic energy converts into the generating process of internal tides (baroclinic). The result of baroclinic energy will be dissipated locally or radiated to the open ocean.

4. Conclusions

The problem of internal waves in the ocean can be illustrated by the basic fluid equation. The mathematical representation of the basic fluid equation is a system of nonlinear partial differential equations that are difficult to solve analytically. Homotopy method has been succesfully applied in finding the approximate solution of the internal wave model. Solutions by this methods are then compared with one of numerical method. The use of HAM in the solution to basic fluid equations is efficient and simple, since it involves only modest calculations using the common integral.

Data Availability

All data used for this study are publicly available. No new data were created during this study.

Conflicts of Interest

The authors declare that there are no conflicts of interest regarding the publication of this paper.

References

[1] A. R. Osborne and T. L. Burch, "Internal solitons in the Andaman Sea," *Science*, vol. 208, no. 4443, pp. 451–460, 1980.

[2] D. Yang, H. Ye, and G. Wang, "Impacts of internal waves on chlorophyll a distribution in the northern portion of the South China Sea," *Chinese Journal of Oceanology and Limnology*, vol. 28, no. 5, pp. 1095–1101, 2010.

[3] Y. Cuypers, B. Vinçon-Leite, A. Groleau, B. Tassin, and J.-F. Humbert, "Impact of internal waves on the spatial distribution of Planktothrix rubescens (cyanobacteria) in an alpine lake," *The ISME Journal*, vol. 5, no. 4, pp. 580–589, 2011.

[4] T. T. Warner, *Numerical Weather and Climate Prediction*, Cambridge University Press, Cambridge, UK, 2011.

[5] S. J. Liao, "Beyond Perturbation," in *Introduction to Homotopy Analysis Method*, pp. 296–309, A CRC Press Company, New york, NY, USA, 2004.

[6] A. K. Alomari, M. S. Noorani, and M. S. Roslinda, "Approximate analytical solutions of the Klein-Gordon equation by means of the homotopy analysis method," *Journal of Quality Measurement and Analysis*, vol. 4, pp. 45–57, 2008.

[7] J. Mo, W. Lin, and H. Wang, "A class of homotopic solving method for ENSO model," *Acta Mathematica Scientia B*, vol. 29, no. 1, pp. 101–110, 2009.

[8] K. M. Hemida and M. S. Mohamed, "Numerical simulation of the generalized Huxley equation by homotopy analysis method," *Journal of Applied Functional Analysis*, vol. 5, no. 4, pp. 344–350, 2010.

[9] M. Usman, T. Zubair, I. Rashid, and et. al, "Modified homotopy analysis method for zakharov-kuznetsov," *Walailak*, vol. 10, pp. 467–478, 2013.

[10] Jaharuddin, "A single species population model in polluted environment solved by homotopy analysis method," *Applied Mathematical Sciences*, vol. 8, no. 17-20, pp. 951–961, 2014.